Targeting, isertion and localization of E. coli YidC.

Urbanus, M.L.; Froderberg, L.; Drew, D; Bjork, P; de Gier, J.-W.; Brunner, J; Oudega, B.; Luirink, S.

published in
Journal of Biological Chemistry
2002

DOI (link to publisher)
10.1074/jbc.M200311200

document version
Publisher's PDF, also known as Version of record

THE JOURNAL OF BIOLOGICAL CHEMISTRY
Vol. 277, No. 15, Issue of April 12, pp. 12718–12723, 2002
Printed in U.S.A.

Targeting, Insertion, and Localization of *Escherichia coli* YidC*

Received for publication, January 11, 2002, and in revised form, January 28, 2002
Published, JBC Papers in Press, January 30, 2002, DOI 10.1074/jbc.M200311200

Malene L. Urbanus‡§, Linda Fröderberg§¶, David Drew¶, Petra Björk¶, Jan-Willem L. de Gier¶, Josef Brunner‖, Bauke Oudega‡, and Joen Luirink‡

From the ‡Department of Microbiology, Institute for Molecular Biological Sciences, De Boelelaan 1087, 1081 HV Amsterdam, The Netherlands, the ¶Department of Biochemistry, Biophysics, and Molecular Biology, Stockholm University, S-106 91 Stockholm, Sweden, and the ‖Institute for Biochemistry, Swiss Federal Institute of Technology Zurich, CH-8093 Zürich, Switzerland

YidC was recently shown to play an important role in the assembly of inner membrane proteins (IMPs) both in conjunction with and separate from the Sec-translocon. Little is known about the biogenesis and structural and functional properties of YidC, itself a polytopic IMP. Here we analyze the targeting and membrane integration of YidC using *in vivo* and *in vitro* approaches. The combined data indicate that YidC is targeted by the signal recognition particle and inserts at the SecAYEG-YidC translocon early during biogenesis, unlike its mitochondrial homologue Oxa1p. In addition, YidC is shown to be relatively abundant compared with other components involved in IMP assembly and is predominantly localized at the poles of the cell.

In *Escherichia coli*, inner membrane protein (IMP)[1] integration can occur via Sec-dependent or Sec-independent mechanisms (1). The majority of IMPs are targeted to the membrane by the signal recognition particle (SRP) and its receptor FtsY that mediates co-translational targeting to the Sec-translocon (2). The SRP, which consists of the 4.5 S RNA and Ffh (for fifty-four homologue) is homologous to the eukaryotic SRP but less complex in composition. The core Sec-translocon consists of the integral membrane components SecY, SecE and SecG, which form a heterotrimer, and the peripheral subunit SecA (3). The translocon serves as a translocating pore for both secretory proteins and IMPs. SecA is an ATPase that functions as a molecular motor that drives the translocation of secretory proteins and large periplasmic domains of IMPs through the SecYEG pore.

Recent evidence shows that a novel component, YidC, is specifically involved in Sec-dependent IMP integration (4). Using a site-specific photocross-linking procedure, YidC was shown to interact with the nascent IMPs, FtsQ, Lep, and mannitol permease, as they move laterally from the Sec-translocon into the lipid bilayer (5–8). This interaction appeared to be specific for the transmembrane segments (TMs) in the nascent polypeptide. Moreover, YidC could be co-purified with the Sec-translocon suggesting a physical connection (7). Upon depletion of YidC, the assembly of Sec-dependent IMPs such as Lep and FtsQ is hampered, although the effect is relatively mild (8, 9).

In contrast to most IMPs, some small phage coat proteins (like Pf3 coat and M13 procoat proteins) insert into the inner membrane independent of the Sec-translocon (10). These proteins were considered to partition spontaneously into the lipid bilayer (*i.e.* without the requirement of any proteinaceous factors and only depending on the proton motive force to energize the process). However, it was recently demonstrated that membrane assembly of M13 coat protein is almost completely blocked upon depletion of YidC suggesting a crucial role for YidC in the integration of Sec-independent proteins (9, 11).

YidC is homologous to the mitochondrial IMP Oxa1p and to the thylakoid membrane protein Alb3, which both have been implicated in membrane protein integration (4). Oxa1p is essential for the correct insertion of a subset of both mitochondrial-encoded IMPs (like pCoxII) and nuclear-encoded IMPs (like Oxa1p itself). Interestingly, mitochondria do not have an SRP-like targeting pathway or a Sec-like translocon suggesting that Oxa1p might function in a fashion similar to YidC in the Sec-independent route.

YidC is a polytopic IMP that spans the membrane six times with an N-in, C-in topology and a large, poorly conserved periplasmic domain between TM1 (signal anchor sequence) and TM2 (Fig. 2*A*) (12). As is true for most polytopic IMPs, hardly anything is known about the targeting, assembly, localization, and cellular abundance of YidC. Here, we present evidence that YidC is targeted co-translationally by the SRP to the Sec-translocon, which appears to be required for proper assembly. Nascent YidC is shown to contact SecA, SecY, and pre-existing YidC very early during biosynthesis. YidC is found to be present in excess over SecYEG. Finally, using GFP fusion technology we found that YidC accumulates at the poles of the cell.

EXPERIMENTAL PROCEDURES

Materials—Restriction enzymes, Expand long template PCR system, and Lumi-Light^{PLUS} Western blotting substrate were from Roche Molecular Biochemicals. Megashort script T7 transcription kit was from Ambion Inc. [^{35}S]methionine and protein A-Sepharose were from Amersham Biosciences. T4 Ligase and T4 DNA polymerase were from Epicentre Technologies. All other chemicals were supplied by Sigma. Antiserum against a C-terminal peptide of YidC has been described previously (7). In addition, an antiserum against purified hisYidC (see below) was raised in rabbit by Agrisera (Umeå, Sweden). The antisera directed against Trigger Factor (TF) and SecA were gifts from W. Wickner, and anti-SecY was a gift from A. Driessen.

* This work was supported by grants from the European Community (to J. L.), the European Molecular Biology Organization (European Molecular Biology Young Investigators Program), the Swedish Foundation for Strategic Research, the Swedish Research Council and the Carl Trygger Foundation (to J.-W.L.G.), and the Swiss National Science Foundation (to J. B.). The costs of publication of this article were defrayed in part by the payment of page charges. This article must therefore be hereby marked "*advertisement*" in accordance with 18 U.S.C. Section 1734 solely to indicate this fact.

§ These authors contributed equally to this work.

** To whom correspondence should be addressed: Dept. of Microbiology, Institute of Molecular Biological Sciences, De Boelelaan 1087, 1081 HV, Amsterdam, The Netherlands. Tel.: 31-20-4447175; Fax: 31-20-4446979.

[1] The abbreviations used are: IMP, inner membrane protein; SRP, signal recognition particle; Ffh, fifty-four homologue; TM, transmembrane segments; GFP, green fluorescent protein; TF, Trigger Factor; LB, Luria Bertani; IPTG, isopropyl-1-thio-β-D-galactopyranoside; IMV, inverted inner membrane vesicles.

Strain and Plasmids—*E. coli* strain MRE600 was used to prepare a lysate for translation of *in vitro* synthesized mRNA and suppression of UAG stop codons in the presence of (Tmd)Phe-tRNA^{sup}. Strain MC4100 grown in Luria Bertani (LB) medium was used to isolate inverted membrane vesicles (IMVs) and as an expression host for plasmid pEH1hisYidC (overexpression of YidC carrying a hexahistidine tag)(13). The *E. coli* strain JS7131 in which *yidC* is under the control of the *araBAD* operator/promoter (9) was used to study the complementation of YidC depletion by expression of YidC-GFP. The 4.5 S RNA conditional strain FF283 and the SecE depletion strain CM124 were cultured and depleted as described previously (14–16). The conditional SecA strain BA13 and its control strain DO251 were cultured and depleted for SecA essentially as described (17, 18). The SecG deletion strain KN370 (19) was cultured in M9 minimal medium to the mid-exponential growth phase as described previously (16). Plasmid p*H*+ (20) was used to complement the SecG deletion strain KN370 with SecG. Plasmid pEH1YidC, harboring *yidC* under control of a *lac* promoter, was constructed in a 3-step procedure as follows. First, the 5′-region of *yidC* was cloned *Nco*I-*Kpn*I from pAra14-YidC (7) in the pEH1 vector. Second, using pAra14-YidC as a template a *Sma*I site was introduced downstream of *yidC* by PCR. Subsequently, the 3′ *yidC* fragment was cloned *Kpn*I-*Sma*I in pEH1YidC*Nco*I-*Kpn*I to generate full-length *yidC*. For YidC-GFP expression, YidC was fused at its C terminus to the N terminus of a GFP variant that has been selected to fold well in *E. coli* (21). The YidC-GFP fusion was cut out with *Xba*I-*Hin*dIII from plasmid pWaldoYidC-GFP and cloned *Xba*I-*Sma*I (the *Hin*dIII site of the DNA fragment harboring the YidC-GFP fusion was made blunt using T4 DNA polymerase) into the pEH1 expression vector yielding pEH1YidC-GFP. Plasmids pC4meth52YidCTAG17 and pC4Meth96YidCTAG17 were obtained by PCR using pEH1YidC as a template. They encode truncated YidC fused to a C-terminal 4× methionine tag to improve the labeling efficiency and contain an amber mutation at position 17 to enable sup-tRNA photocross-linking (see below). The nucleotide sequences of all cloned mutant genes were confirmed by DNA sequencing.

In Vitro Transcription, Translation, Targeting, and Cross-linking—Truncated mRNA was prepared as described previously (7) from *Hin*dIII-linearized pC4Meth52YidCTAG17 or pCMeth96YidCTAG17. For photocross-linking, (Tmd)Phe was site-specifically incorporated into YidC nascent chains by suppression of a UAG stop codon using (Tmd)-Phe-tRNA^{sup} in an *E. coli in vitro* translation system containing [^{35}S]methionine to label the nascent chains. This procedure has been described previously (7, 8). Targeting to IMVs, photocross-linking and carbonate extraction (to separate soluble and pheriperal membrane proteins from integral membrane proteins) were carried out as described previously (7). Carbonate soluble and insoluble fractions were either trichloracetic acid-precipitated or immunoprecipitated. The material used for immunoprecipitation was 4-fold the amount used for trichloracetic acid precipitation. Sample analysis (SDS-PAGE and phosphorimaging) was as described previously (7).

In Vivo Assay for Membrane Assembly—Strains FF285, BA13, DO251, CM124, and KN370 were grown to the mid-exponential phase of growth. Expression of YidC was induced for 3 min with either 1 mM IPTG (from pEH1YidC in strain CM124) or 0.2% L-arabinose (from pAra14-YidC in the strains FF283, BA13, DO251, and KN370). Aliquots were pulse-labeled for 30 s with 150 μCi of [^{35}S]methionine and converted to spheroplasts as described previously (16). Aliquots of the spheroplast suspensions were incubated on ice for 1 h in the presence or absence of proteinase K (0.3 mg/ml). Subsequently, phenylmethylsulfonyl fluoride was added to the spheroplast suspensions (0.33 mg/ml) to inhibit the protease. Finally, the samples were precipitated in 10% trichloracetic acid and immunoprecipitated with antisera against YidC, OmpA, or AraB/BandX and analyzed using SDS-PAGE.

Estimation of the Number of YidC Molecules per Cell—The cellular abundance of YidC was determined essentially as described (22). An overnight culture of MC4100 was diluted 1:100 in LB medium and grown at 37 °C to the mid-exponential phase of growth. Cells were harvested and diluted for life cell counts by plating on LB-agar. From the remainder of the samples a range of 0.05–0.0025 OD_{660} units of cells was analyzed using SDS-PAGE and Western blotting next to a 1–20-ng standard of purified hisYidC. The blots were incubated with antibodies directed against hisYidC and developed using Lumi-Light^{PLUS} Western blotting substrate. The chemiluminescent signal was detected using the Fluor-S MultiImager (Bio-Rad) and quantified using Multi-Analyst 1.0.2 software (Bio-Rad). HisYidC was purified from Top10F′ containing pEH1hisYidC as described previously (13). Protein concentration was determined using the D_C protein assay (Bio-Rad) and bovine serum albumin as a standard.

Expression and Localization of YidC-GFP—YidC-GFP was expressed in the conditional YidC depletion strain JS7131. Cells were grown for 6 h at 37 °C in LB medium supplemented with 0.2% L-arabinose (to generate non-depleted control cells) or 10 μM IPTG (to deplete for YidC and express YidC-GFP). Cells were then harvested and used for analysis of YidC/YidC-GFP expression and fluorescence microscopy. To monitor YidC and YidC-GFP expression, cells were washed with M9 minimal medium and resuspended in M9 minimal medium supplemented with 0.2% L-arabinose or 10 mM IPTG. Subsequently, the cells were labeled for 1 h with [^{35}S]methionine (150 μCi/ml), trichloracetic acid-precipitated, washed with cold acetone, and resuspended in 10 mM Tris-HCl pH 8.0/2% SDS. YidC and YidC-GFP were immunoprecipitated with anti-YidC serum and analyzed by SDS-PAGE. For localization of YidC-GFP, cells expressing YidC-GFP were harvested and resuspended in 50 mM Tris-HCl pH 8.0, 200 mM NaCl, 15 mM EDTA. GFP fluorescence was viewed with an Axioplan 2 microscope (Zeiss) equipped with a filter set for fluorescein isothiocyanate. Images were captured using a CCD camera (Color Cool View, Photonic Sciences) and Image Pro-Plus software.

RESULTS

Nascent YidC Interacts with SecY and YidC—We analyzed the pathway of targeting and membrane insertion of nascent YidC (a polytopic IMP) using an *in vitro* translation/targeting/photocross-linking assay that we initially developed for the analysis of molecular interactions during biosynthesis of the less complex IMPs, FtsQ and Lep (6, 7).

Radiolabeled nascent chains of YidC of 52 and 96 amino acids were synthesized by translation of truncated mRNA in a membrane-free *E. coli* extract in the presence of [^{35}S]methionine. Purified inverted IMVs were added from the start of the translation reaction to allow co-translational membrane targeting and insertion of the translation intermediates. To specifically probe the molecular environment of the first TM, a stop codon (TAG) was introduced at position 17 in the center of the TM region and suppressed during *in vitro* synthesis by the addition of (Tmd)Phe-tRNA^{sup} that carries a photoreactive probe. After the translation/insertion reaction, one-half of each sample was irradiated with UV light to induce cross-linking whereas the other half was kept in the dark to serve as a control. The samples were extracted with carbonate to separate untargeted material from the membrane-integrated material, and cross-linking partners were identified by immunoprecipitation.

In both constructs, the TAG17 mutation was efficiently suppressed by (Tmd)Phe-tRNA^{sup} (data not shown), resulting in nascent YidC of the expected apparent molecular weight. Assuming that the ribosome covers ~35 amino acids, the 52-mer only partially exposes the TM outside the ribosome, and the photocross-linking group is just exposed outside the ribosome (Fig. 1*A*). Using this construct, a major cross-linking adduct of ~60 kDa was observed in the untargeted (carbonate soluble) nascent chains (Fig. 1*B*, *lanes 1* and *2*). Immunoprecipitation identified TF as the cross-linking partner (Fig. 1*B*, *lane 3*). Furthermore, two less prominent cross-linking adducts of ~55 and ~100 kDa were identified as Ffh, the protein component of the SRP, and SecA (Fig. 1*B*, *lanes 4* and *5*). Anti-Ffh also precipitated smaller adducts that might represent degradation products. The 52-mer was less efficiently integrated in the membrane than the longer YidC construct as judged by the criterion of carbonate resistance (~25% *versus* ~45%, not shown). Membrane-integrated 52-mer gave rise to distinct cross-linking adducts of ~40, ~60, and ~100 kDa (Fig. 1*B*, *lanes 6* and *7*), which were immunoprecipitated with anti-SecY, anti-YidC, and anti-SecA, respectively (Fig. 1*B*, *lanes 8–10*). For identification of nascent YidC-YidC adducts, antiserum raised against the C terminus of YidC was used to distinguish full-length YidC from nascent YidC. A fourth cross-linking adduct of ~55 kDa was not immunoprecipitated with any of the antisera used and remains to be identified.

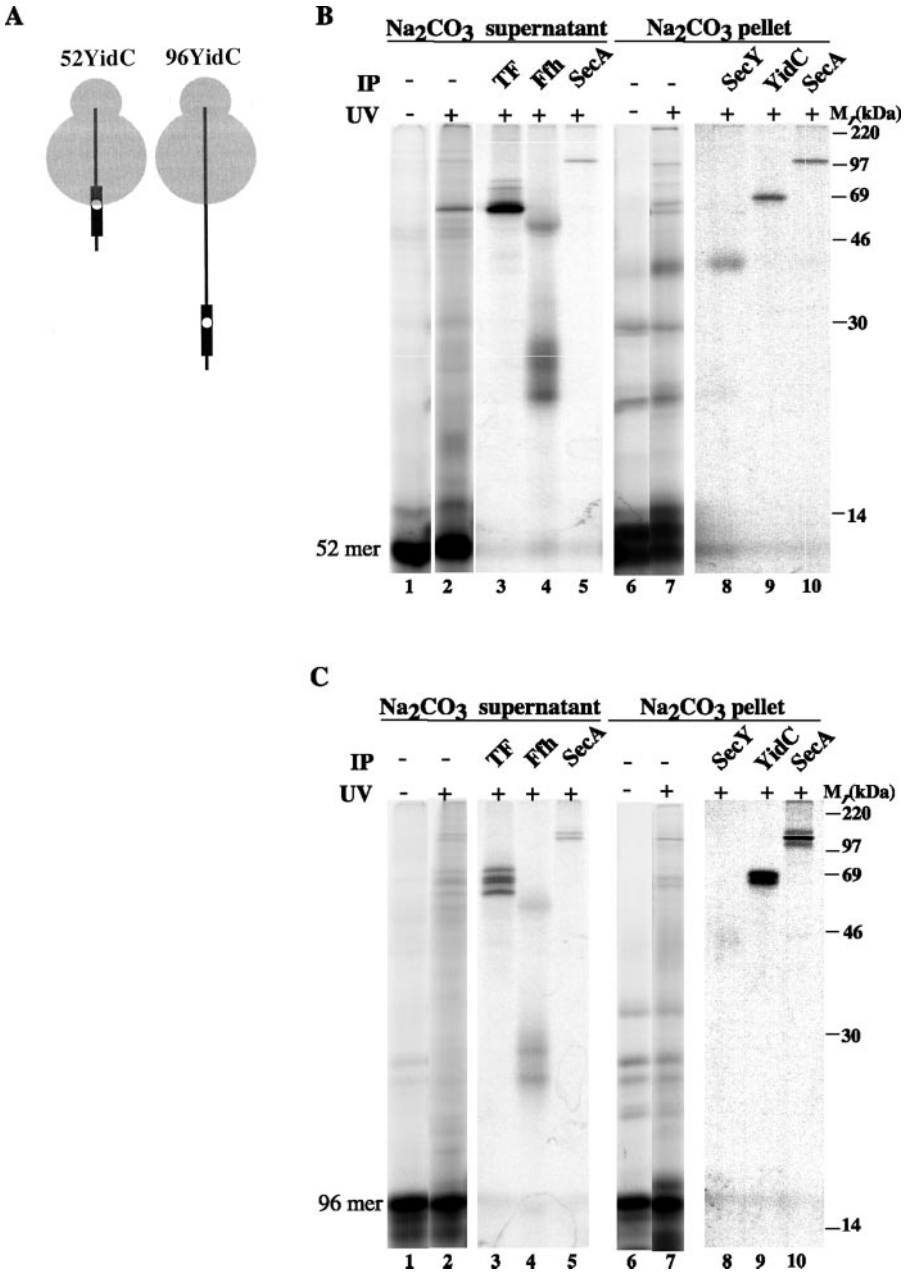

FIG. 1. **Interactions of nascent YidC.** *A*, nascent YidC species used in this study. The TM region is represented by a *thick line* with a *white dot* at the position of the photocross-linking probe. *B* and *C*, *in vitro* synthesis of nascent 52YidC (*B*) and 96YidC (*C*) with a TAG codon at position 17 was carried out in the presence of IMVs and (Tmd)Phe-tRNA^{sup}. After translation, samples were kept in the dark or UV-irradiated and subsequently extracted with carbonate (supernatant, *lanes 1–5*; pellet, *lanes 6–10*). UV-irradiated fractions were immunoprecipitated using antiserum against TF, Ffh, SecA, SecY, and the C terminus of YidC (*lanes 3–5* and *8–10*). The translation products at 30–40 kDa present in *lanes 6* and *7* represent the peptidyl-tRNA form of nascent YidC.

In the longer 96-mer, the TM and ~38 residues of the first periplasmic domain are exposed outside the ribosome (Fig. 1*A*). Untargeted nascent chains still cross-linked to TF, giving rise to several distinct adducts possibly caused by the binding of TF at several positions in this longer nascent chain (23). Ffh and SecA were cross-linked but to a lesser extent than with the shorter nascent chains (Fig. 1*C*, *lanes 1–5*). The membrane-integrated nascent chains showed predominantly cross-linking to YidC and SecA. SecY was also cross-linked, albeit much less efficiently than with the 52-mer (Fig. 1*C*, *lanes 6–10*).

Taken together, these data show that the first TM in short nascent YidC interacts with TF and SRP and inserts into the inner membrane in a carbonate resistant configuration in the vicinity of pre-existing YidC, SecY, and SecA. The difference in cross-linking efficiencies of the 52-mer and 96-mer to SecY suggests that the first TM of YidC is close to SecY only early during the membrane insertion process.

Efficient Targeting and Assembly of YidC in Vivo Requires SRP, SecYEG, and SecA—We have shown that nascent YidC interacts with Ffh, TF, SecA, SecY, and YidC. To investigate whether these interactions reflect an *in vivo* dependence on the SRP targeting pathway or Sec-translocon for correct membrane assembly of the full-length protein, we monitored the requirements for *in vivo* assembly of YidC in a proteinase K accessibility assay. When YidC is correctly targeted and assembled in the inner membrane, the large periplasmic loop between TM1 and TM2 (Fig. 2*A*) is proteinase K-resistant except for a small region near TM1 (Fig. 2*A*) (12). Consequently, proteinase K treatment of spheroplasts derived from wild-type cells results in a small band shift of YidC in SDS-PAGE (Fig. 2*B*, *lanes 1* and *2*). OmpA and band X are periplasmic and cytoplasmic control proteins, respectively, used to monitor spheroplast formation (24). In addition, proOmpA processing was monitored to check SecA and SecE depletion.

Depletion of 4.5 S RNA, the RNA component of SRP, affected the assembly of YidC into the inner membrane as is evident from the appearance of full-length YidC in proteinase K-treated spheroplasts (Fig. 2*B*). Depletion of SecA had a similar effect whereas depletion of SecE had an even stronger effect (Fig. 2, *C* and *D*). The SecE depletion strain was used

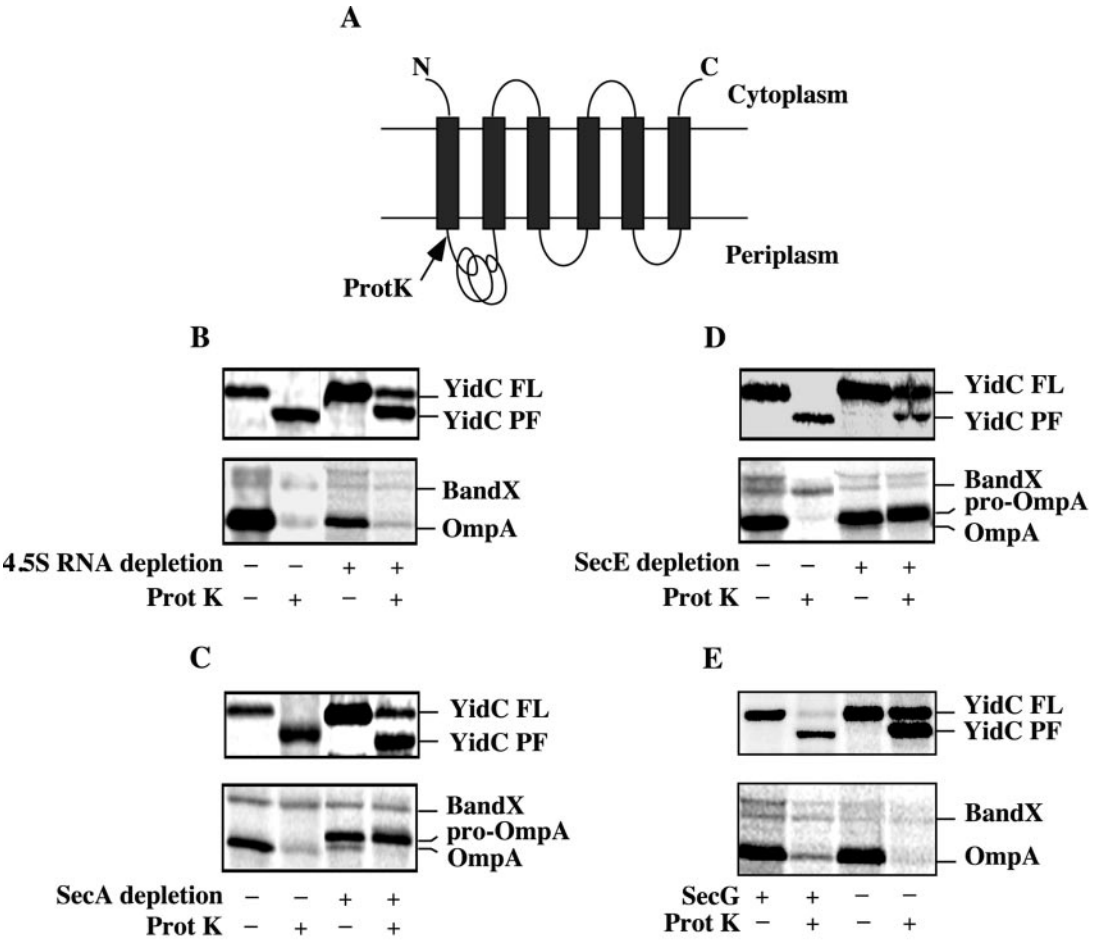

FIG. 2. **Assembly of YidC is dependent on the SRP and the SecAYEG-translocon.** *A*, schematic representation of the topology of YidC. Proteinase K-sensitive site is indicated with *ProtK*. *B*, proteinase K accessibility of YidC (*top*) and OmpA/bandX (*bottom*) in FF283 (4.5 S RNA depletion strain) spheroplasts, prepared from cells grown in the absence or presence of IPTG. Cells were labeled and processed as described under "Experimental Procedures." *C*, proteinase K accessibility in BA13 (SecA depletion strain) and DO251 (control strain) spheroplasts, prepared from cells cultured at 41 °C. *D*, proteinase K accessibility in CM124 (SecE depletion strain) spheroplasts, prepared from cells not depleted and depleted for SecE. *E*, proteinase K accessibility in KN370 (SecG deletion strain) spheroplasts with and without the SecG complementation vector p*H*+. *YidC FL* is the full-length form of YidC, and *YidC PF* is the proteinase K-digested fragment of YidC.

because it enables the most efficient inactivation of the SecYEG core translocon thus far (15). Upon depletion of SecE, SecY is rapidly degraded by the protease FtsH (25). We also monitored the assembly of YidC in a SecG deletion background (Fig. 2*E*). The Sec-translocon component SecG also seems to be required for the efficient assembly of YidC.

Unfortunately, we could not monitor the assembly of YidC in a YidC depletion background because the YidC background expression levels from the plasmid-borne copy of YidC were sufficient to alleviate chromosomal YidC depletion. Taken together, these data confirm the involvement of the SRP, SecA, and SecYEG in the proper targeting and assembly of YidC into the inner membrane.

Abundance of YidC—To determine the abundance of YidC in *E. coli* cells a semiquantitative Western blot procedure was employed. MC4100 was grown to the mid-exponential phase of growth and harvested for life cell counts and analysis by SDS-PAGE and Western blotting. A range of 0.05–0.0025 OD_{660} units of cells was analyzed (Fig. 3). To calculate the amount of YidC from Western blot, the chemiluminescent signal of a standard of purified hisYidC (1–20 ng) was quantified and fitted. A linear relationship between the amount of hisYidC and the chemiluminscent signal was observed throughout this range. The amount of YidC in the cell samples was calculated and correlated to the life cell counts. A MC4100 cell contains ~0.27 fg of YidC corresponding to 2700 copies of YidC per cell.

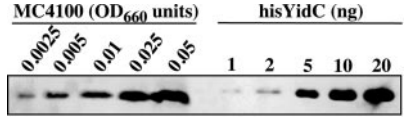

FIG. 3. **Determination of the number of YidC molecules per cell.** A range of 0.05–0.0025 OD_{660} units of MC4100 cells grown to the mid-exponential phase of growth was analyzed using SDS-PAGE and Western blotting next to a 1–20-ng standard of purified hisYidC. YidC was detected using Western blotting as described under "Experimental Procedures."

A duplicate experiment resulted in a similar amount of 2500 copies of YidC per cell (data not shown).

YidC Is Localized at the Poles of the Cell—Where the inner membrane assembly of IMPs occurs has not yet been studied. Because YidC appears to be exclusively involved in IMP insertion and assembly (9), we have studied the spatial localization of YidC in the inner membrane using GFP-tagging technology.

GFP was fused to the C terminus of YidC, and cloned into the IPTG inducible expression vector pEH1. The YidC depletion strain JS7131, in which *yidC* is under the control of the *araBAD* operator/promoter, was transformed with pEH1 (empty control vector) and pEH1YidC-GFP.

To test if the fusion construct was functional, JS7131 (pEH1YidC-GFP) and its control strain JS7131 (pEH1) were plated onto LB-agar plates containing 0.2% L-arabinose (to

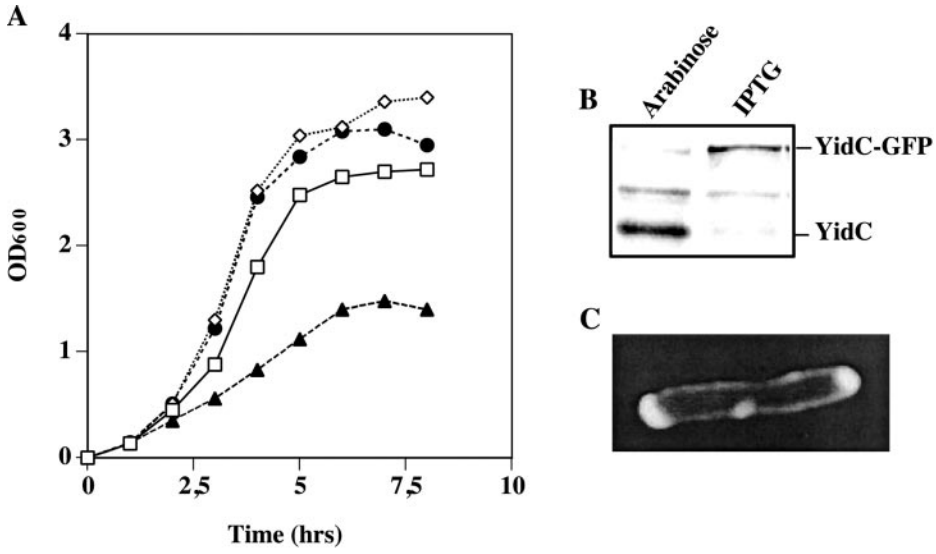

FIG. 4. **Localization of functional YidC-GFP.** *A*, complementation of YidC depletion with the YidC-GFP fusion protein. JS7131 cells carrying the YidC-GFP expression vector pEH1YidC-GFP or the empty expression vector pEH1, were grown in LB medium supplemented with 0.2% L-arabinose (to generate non-depleted control cells) or 10 μM IPTG (to deplete wild-type YidC and express YidC-GFP). Growth was monitored by measuring the OD_{600}. JS7131 (pEH1) grown in the presence of L-arabinose (●) or IPTG (▲) and JS7131 (pEH1YidC-GFP) grown in the presence of L-arabinose (◇) or IPTG (□) are indicated. *B*, to monitor the levels YidC and YidC-GFP expression, an overnight culture grown in the presence of both L-arabinose and IPTG, was diluted in fresh medium, and grown for 6 h in the presence of either 0.2% L-arabinose or 10 μM IPTG. The cells were harvested and transferred to M9 minimal medium and labeled with [^{35}S]methionine for 1 h. YidC and YidC-GFP were immunoprecipitated using antiserum against the C terminus of YidC and analyzed using SDS-PAGE and phosphorimaging. *C*, localization of YidC-GFP. Cells were grown as described under *B*, and then harvested and visualized with the fluoresence microscope as described under "Experimental Procedures."

generate non-depleted control cells) or 0.2% glucose (to generate YidC-depleted cells). Because YidC is essential for growth, the control strain JS7131(pEH1) could not grow in the absence of L-arabinose. In contrast, JS7131 (pEH1YidC-GFP) grew in the presence and absence of L-arabinose without any discernable differences (data not shown). These observations demonstrate that even at uninduced expression levels, leaky expression of the plasmid-encoded YidC-GFP is able to complement depletion of YidC. However, in liquid culture uninduced JS7131 (pEH1YidC-GFP) grows slightly slower than JS7131 (pEH1) grown in the presence of 0.2% L-arabinose. An additional induction with 10 μM IPTG was required for optimal growth (Fig. 4*A*). The expression of YidC-GFP was monitored by labeling JS7131 (pEH1YidC-GFP) cells grown either in the presence of 0.2% L-arabinose or 10 μM IPTG with [^{35}S]methionine and subsequent immunoprecipitation using antiserum to YidC (Fig. 4*B*). Cells in which the chromosomal *yidC* but not the plasmid *yidC-GFP* copy was expressed contained only a trace amount of YidC-GFP and a normal amount of YidC, whereas in YidC-depleted/YidC-GFP-induced cells only YidC-GFP could be detected at a level comparable with chromosome encoded YidC. Taken together, these data unambiguously show that the YidC-GFP fusion is functional. In addition, cell fractionation studies indicated that both YidC and YidC-GFP are membrane-associated (data not shown).

To visualize YidC-GFP in living cells, cells of strain JS7131 (pEH1YidC-GFP) were grown in LB medium in the presence of 10 μM IPTG to express the fusion protein. Cells from different growth stages were inspected by fluorescence microscopy. Surprisingly, at all growth stages fluorescence was concentrated at the poles of the JS7131(pEH1YidC-GFP) cells, indicating that YidC-GFP is predominantly localized at the poles of the cell (Fig. 4*C*). As an additional control, other polytopic IMPs were fused to GFP and expressed at physiological levels. In contrast to YidC-GFP, fluorescence of all tested IMPs was distributed uniformly over the inner membrane (data not shown), indicating that the localization of YidC-GFP is specific for YidC and not an artifact caused by the fusion to GFP.

DISCUSSION

So far, the biogenesis of *E. coli* IMPs has been studied using only a very limited set of model IMPs (1). Among these model IMPs there are hardly any complex polytopic IMPs. Here we analyze the biogenesis of YidC, a polytopic IMP that has recently attracted attention as a factor that might play a key role in the membrane integration and assembly of *E. coli* IMPs (7, 9). Using a combined *in vitro* and *in vivo* approach we provide evidence that the polytopic IMP YidC follows the SRP/Sec-translocon/YidC pathway for its membrane integration. In addition, we show that YidC is predominantly localized at the cell poles with an abundance of ~2500–3000 copies per cell.

Recently, we have analyzed the pathway of targeting and membrane insertion of the bitopic model IMP FtsQ by studying the sequential interactions of nascent FtsQ in the cytosol and membrane in an *in vitro* photocross-linking assay. This revealed a sequential interaction of the TM, first with SecY and then with YidC (8). The most prominent SecY interaction was found when the TM was only partially exposed outside of the ribosome, whereas the strongest YidC interaction was found when the TM and ~25–30 residues of the periplasmic domain were exposed outside the ribosome. In this study, two YidC constructs were used (52YidC and 96YidC) that resemble these two FtsQ constructs with respect to the distance between the ribosome and the TM and carry a photocross-linking probe in the exposed TM1 region (Fig. 1*A*).

In contrast to FtsQ, the cross-linking to YidC appears rather complex. The early interaction of nascent YidC with SecY that is almost absent in the longer construct is comparable with the transient interaction of nascent FtsQ with SecY. Different from FbQ are the early interactions with pre-existing YidC and SecA that both persist and even increase in the longer construct. This might indicate that YidC inserts close to SecY/SecA/YidC in a flexible environment that is shielded from water given the sensitivity of the cross-linking probe to quenching by water.

The mechanism of membrane insertion of polytopic IMPs may not be generic. The sugar co-transporter melibiose per-

mease has been claimed (26) to insert completely independently from the Sec machinery, whereas mannitol permease inserts at SecYE but does not require SecA nor SecG (27, 28). It has been suggested that SecA only plays a role in the translocation of large periplasmic loops that are not present in mannitol permease (29). YidC does contain a large periplasmic loop between TM1 and TM2, which might explain its dependence on SecA (Ref. 12 and this study). Remarkably, SecA is cross-linked to TM1 in 52YidC, which does not expose any periplasmic sequence. It remains to be determined how the future requirement for SecA is sensed in such short nascent chains.

Interestingly, the absence of SecG strongly affected YidC assembly, whereas the deletion of SecG only affects protein secretion at low temperatures (19), and SecG has not previously been implicated in membrane protein assembly. The effect on YidC assembly may be related to the proposed function of SecG in the modulation of the SecA cycle of membrane insertion and deinsertion (31). Alternatively, SecG may be specifically involved in connecting YidC to the core SecYE translocon thus indirectly influencing YidC assembly.

Apparently, YidC inserts via the SRP/Sec-translocon/YidC pathway. In contrast, the mitochondrial YidC homologue Oxa1p assembles solely at Oxa1p itself in the absence of SRP and Sec homologues (32). This may be related to the different topology of Oxa1p, which lacks the first TM of YidC (4).

In the cytosolic fraction 52YidC is cross-linked to both SRP (consistent with the *in vivo* dependence on SRP) and TF. This confirms the very early interaction of TF with nascent chains as observed previously for PhoE (23). It has been suggested that TF specifically interacts with the early mature region of secretory proteins to prevent interaction with the SRP and funnel the proteins into the SecB/SecA targeting route (33). Our observations are not consistent with a restricted role for TF in secretion. Apparently, TF is well able to interact with the TM sequence of a nascent IMP. We propose that TF is juxtaposed to all nascent sequences near the ribosome exit site, whereas SRP displaces TF when the exposed region is of sufficient hydrophobicity (Ref. 34 and this study).

Surprisingly, the *E. coli* strain MC4100 contains ~2500–3000 copies of YidC per cell. The core translocon components SecY and SecE occur with ~300–600 and 200–400 copies per cell, respectively (30). Components of the accessory complex SecDFYajC are even less abundant with ~30–100 copies per cell (30). Assuming that SecYEG tetramers form functional translocation units, a cell contains ~100–200 functional translocons. Hence, YidC appears to be in excess, arguing against an exclusive association with the SecYEG translocon even when YidC would be dimeric (13). This may be related to the dual function of YidC: in conjunction with the Sec-translocon and as a separate entity.

YidC is a *bona fide* IMP spanning the membrane six times with short cytoplasmic N and C termini (12). Intriguingly, fusion of the C terminus to GFP did not affect the functioning of YidC and revealed a predominant localization at the poles of the *E. coli* cell. At present it is too early to speculate whether the cell poles function as dedicated IMP insertion sites perhaps related to the high membrane curvature in this region. We will investigate whether other Sec-translocon components colocalize with YidC at the cell poles using the GFP-tagging and Fluorescence Resonance Energy Transfer technology.

Acknowledgment—We thank C. M. ten Hagen-Jongman for technical support.

REFERENCES

1. de Gier, J.-W., and Luirink, J. (2001) *Mol. Microbiol.* **40,** 314–322
2. Herskovits, A. A., Bochkareva, E. S., and Bibi, E. (2000) *Mol. Microbiol.* **38,** 927–939
3. Manting, E. H., and Driessen, A. J. M. (2000) *Mol. Microbiol.* **37,** 226–238
4. Luirink, J., Samuelsson, T., and de Gier, J.-W. (2001) *FEBS Lett.* **1,** 1–5
5. Beck, K., Eisner, G., Trescher, D., Dalbey, R. E., Brunner, J., and Müller, M. (2001) *EMBO Rep.* **2,** 709–714
6. Houben, E. N. G., Scotti, P. A., Valent, Q. A., Brunner, J., de Gier, J.-W., Oudega, B., and Luirink, J. (2000) *FEBS Lett.* **476,** 229–233
7. Scotti, P. A., Urbanus, M. L., Brunner, J., de Gier, J. W., von Heijne, G., van der Does, C., Driessen, A. J., Oudega, B., and Luirink, J. (2000) *EMBO J.* **19,** 542–549
8. Urbanus, M. L., Scotti, P. A., Fröderberg, L., Sääf, A., de Gier, J.-W., Brunner, J., Samuelson, J. C., Dalbey, R. E., Oudega, B., and Luirink, J. (2001) *EMBO Rep.* **6,** 524–529
9. Samuelson, J. C., Chen, M. Y., Jiang, F. L., Möller, I., Wiedmann, M., Kuhn, A., Phillips, G. J., and Dalbey, R. E. (2000) *Nature* **406,** 637–641
10. Dalbey, R. E., and Kuhn, A. (2000) *Ann. Rev. Cell Dev. Biol.* **16,** 51–87
11. Samuelson, J. C., Jiang, F., Yi, L., Chen, M., de Gier, J.-W., Kuhn, A., and Dalbey, R. E. (2001) *J. Biol. Chem.* **16,** 16
12. Sääf, A., Monne, M., de Gier, J.-W., and von Heijne, G. (1998) *J. Biol. Chem.* **273,** 30415–30418
13. van der Laan, M., Houben, E. N. G., Nouwen, N., Luirink, J., and Driessen, A. J. M. (2001) *EMBO Rep.* **21,** 519–523
14. Ribes, V., Römisch, K., Giner, A., Dobberstein, B., and Tollervey, D. (1990) *Cell* **63,** 591–600
15. Traxler, B., and Murphy, C. (1996) *J. Biol. Chem.* **271,** 12394–12400
16. de Gier, J.-W., Scotti, P. A., Sääf, A., Valent, Q. A., Kuhn, A., Luirink, J., and von Heijne, G. (1998) *Proc. Natl. Acad. Sci. U. S. A.* **95,** 14646–14651
17. Oliver, D. B., and Beckwith, J. (1982) *Cell* **30,** 311–319
18. Qi, H. Y., and Bernstein, H. D. (1999) *J. Biol. Chem.* **274,** 8993–8997
19. Nishiyama, K., Hanada, M., and Tokuda, H. (1994) *EMBO J.* **13,** 3272–3277
20. Bost, S., and Belin, D. (1997) *J. Biol. Chem.* **272,** 4087–4093
21. Drew, D. E., von Heijne, G., Nordlund, P., and de Gier, J.-W. (2001) *FEBS Lett.* **2,** 220–224.)
22. van Klompenburg, W., Whitley, P., Diemel, R., von Heijne, G., and de Kruijff, B. (1995) *Mol. Membr. Biol.* **12,** 349–353
23. Valent, Q. A., de Gier, J.-W., van Heijne, G., Kendall, D. A., ten Hagen-Jongman, C. M., Oudega, B., and Luirink, J. (1997) *Mol. Microbiol.* **25,** 53–64
24. de Gier, J.-W., Mansournia, P., Valent, Q. A., Phillips, G. J., Luirink, J., and von Heijne, G. (1996) *FEBS Lett.* **399,** 307–309
25. Kihara, A., Akiyama, Y., and Ito, K. (1995) *Proc. Natl. Acad. Sci. U. S. A.* **92,** 4532–4536
26. Bassilana, M., and Gwizdek, C. (1996) *EMBO J.* **15,** 5202–5208
27. Koch, H.-G., Hengelage, T., Neumann-Haefelin, C., MacFarlane, J., Hoffschulte, H. K., Schimz, K.-L., Mechler, B., and Müller, M. (1999) *Mol. Biol. Cell* **10,** 2163–2173
28. Koch, H. G., and Müller, M. (2000) *J. Cell Biol.* **150,** 689–694
29. Neumann-Haefelin, C., Schäfer, U., Müller, M., and Koch, H. G. (2000) *EMBO J.* **19,** 6419–6426
30. Driessen, A. J. M. (1994) *J. Membr. Biol.* **142,** 145–159
31. Nishiyama, K. I., Suzuki, T., and Tokuda, H. (1996) *Cell* **85,** 71–81
32. Hell, K., Herrmann, J. M., Pratje, E., Neupert, W., and Stuart, R. A. (1998) *Proc. Natl. Acad. Sci. U. S. A.* **95,** 2250–2255
33. Beck, K., Wu, L. F., Brunner, J., and Müller, M. (2000) *EMBO J.* **19,** 134–143
34. Lee, H. C., and Bernstein, H. D. (1998) *Proc. Natl. Acad. Sci. U. S. A.* **6,** 3471–3476